

# A WAXD and Solid-State NMR Study on Cocrystallization in Partially Cycloaliphatic Polyamide 12.6-Based Copolymers

Bert Vanhaecht,<sup>†</sup> Rudolph Willem,<sup>‡</sup> Monique Biesemans,<sup>‡</sup> Bart Goderis,<sup>§</sup>  
Monika Basiura,<sup>§</sup> Pieter C. M. M. Magusin,<sup>⊥</sup> Igor Dolbnya,<sup>#</sup> and Cor E. Koning<sup>\*,†,⊥</sup>

Department of Physical and Colloidal Chemistry, Free University of Brussels (VUB), Pleinlaan 2, 1050 Brussels, Belgium; High-Resolution NMR Centre, Free University of Brussels (VUB), Pleinlaan 2, 1050 Brussels, Belgium; Chemistry Department, Catholic University of Leuven, Celestijnenlaan 200F, B-3001 Heverlee, Belgium; Laboratory of Inorganic Chemistry and Catalysis, Eindhoven University of Technology, P.O. Box 513, 5600MB Eindhoven, The Netherlands; DUBBLE-CRG/ESRF, Rue des Martyrs 156, B.P. 220, F-38043 Grenoble Cedex, France; and Laboratory of Polymer Chemistry, Eindhoven University of Technology, P.O. Box 513, 5600MB Eindhoven, The Netherlands

Received July 30, 2003; Revised Manuscript Received November 18, 2003

**ABSTRACT:** To study the influence of the stereochemistry on the possibility of cocrystallization of linear and cyclic aliphatic residues in copolyamides, a series of copolyamides 12.6/12.1,4-cyclohexanedicarboxylic acid with variable compositions were synthesized. From solid-state NMR studies it could be deduced that *cis*-1,4-CHDA is present in the amorphous regions whereas the *trans* residues are located in both the crystalline and the amorphous phase. WAXD patterns confirm the presence of *trans*-1,4-CHDA inside the crystals and reveal that the cycloaliphatic ring is most likely oriented in a direction perpendicular to the crystal sheets that contain the hydrogen bonds. As a result, the intersheet distance is increased compared to that of polyamide 12.6. Furthermore, the rings prevent the genesis of a pseudo-hexagonal phase above the Brill temperature. Exceptionally, crossing rather than merging of the (100) and the combined (010)–(110) WAXD reflections is observed with increasing temperature, indicating that the intersheet distances increase and become larger than the interchain distances within the hydrogen-bonded sheets before the crystals start to melt. Incorporation of *trans*-1,4-CHDA residues into polyamide 12.6 leads to higher melting temperatures, pointing at cocrystallization in terms of a solid solution rather than as defects. In contrast, a slight melting point depression is observed for copolymers with predominately *cis*-1,4-CHDA residues.

## 1. Introduction

The effect of the incorporation of cycloaliphatic monomers in polyesters and polyamides has been reported quite extensively in the literature.<sup>1–10</sup> In previous publications, we have already discussed the partial substitution of the linear aliphatic residues with 1,4-cyclohexanedicarboxylic acid (1,4-CHDA) and 1,4-diaminocyclohexane (1,4-DACH) in the backbone of polyamide 12.6 and polyamide 4.14, respectively.<sup>11,12</sup> Some preliminary differential scanning calorimetry (DSC) and wide-angle X-ray diffraction (WAXD) results on how copolymerization in the copolyamides 12.6/12.1,4-CHDA (see Figure 1) affects thermal behavior and the crystalline structure, respectively, have been communicated as well.<sup>13,14</sup> In these reports the possibility was coined that the more stretched *trans* configuration of the cycloaliphatic residues can be incorporated into the crystals of polyamide 12.6 and that as a result the melting point of the copolymer is increased compared to that of the homopolymer. In contrast, the more kinky *cis* configuration of the cyclic residues probably cannot be incorporated as the melting points of these copoly-

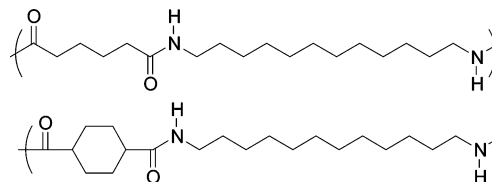


**Figure 1.** Chemical structure of repeating units of copolyamides 12.6/12.1,4-CHDA.

mers do not differ significantly from that of the homopolymer. Up to now no indisputable scientific evidence is available for the mentioned cocrystallization hypotheses. In the present article such evidence is provided, relying on more advanced X-ray characterization and solid-state NMR analysis.

## 2. Experimental Section

**Synthesis and Crystallization of the Copolyamides.** A detailed description of the syntheses with preservation of the stereochemistry of the copolyamides 12.6/12.1,4-CHDA can be found elsewhere.<sup>11,12</sup> Here only a succinct description of the applied low-temperature polycondensation method is given. Under a nitrogen atmosphere 1,12-diaminododecane and triethylamine were dissolved in cold chloroform, after which the desired molar ratio of adipoyl chloride and 1,4-cyclohexanedicarbonyl dichloride, dissolved in chloroform, was added dropwise. After polymerization for 30 min in an acetone/ice cooling bath polymerization was continued at 75 °C for 8 h, after which the residual amine end groups were blocked with an excess of benzoyl chloride. The obtained polyamides were purified by repeated precipitation from formic acid into water and dried under vacuum at 80 °C. It is important to emphasize that all

\* To whom all correspondence should be addressed. E-mail c.e.koning@tue.nl.

<sup>†</sup> Department of Physical and Colloidal Chemistry, VUB.

<sup>‡</sup> High-Resolution NMR Centre, VUB.

<sup>§</sup> Catholic University of Leuven.

<sup>⊥</sup> Laboratory of Inorganic Chemistry and Catalysis, Eindhoven University of Technology.

<sup>#</sup> DUBBLE-CRG/ESRF.

<sup>+</sup> Laboratory of Polymer Chemistry, Eindhoven University of Technology.

solid (semicrystalline) structures of the polyamides discussed in the present work are obtained after synthesis by precipitation from solution into a cold nonsolvent. Hence, crystallization is induced very fast.

**Characterization of the Copolyamides.** Solution  $^1\text{H}$ -decoupled  $^{13}\text{C}$  NMR spectra of the copolyamides dissolved in trifluoroacetic acid/ $\text{CDCl}_3$  (3/1, v/v) were obtained in the inverse-gated Fourier transform mode on a Bruker Avance DRX250 instrument equipped with a Quattro probe tuned to 62.93 and 250.13 MHz for  $^{13}\text{C}$  NMR and  $^1\text{H}$  NMR nuclei (details can be found elsewhere<sup>11,12</sup>). The copolyamide composition and the cis/trans ratio of the cycloaliphatic residues in the polymer main chain were determined from integrated signal areas as obtained by line deconvolution of  $^{13}\text{C}$  NMR resonances using the PERCH TLS (total line shape) software.<sup>15</sup>

With a Cannon-Ubbelohde viscometer intrinsic viscosities of polymer solutions (1.0 g/dL in *m*-cresol) were determined at 25 °C. Size exclusion chromatography was performed with a HP-1090M, equipped with a UV-diode array detector. The solvent/eluent was 1,1,1,3,3,3-hexafluoro-2-propanol (HFIP)/0.2% potassium trifluoroacetate. Polyamide 4.6 and 6 samples with known molecular weight distributions were used as reference samples.

DSC curves were recorded under nitrogen on a Perkin-Elmer DSC 7 at 10 °C/min for both cooling and heating. After first heating the polyamides were kept at 300 °C for 30 min in order to remove all residual crystallites, capable of acting as nucleating agents during cooling. The melting points reported here, taken from the first and second heating curves, refer to the endset values of the endotherms.

The room temperature WAXD (wide-angle X-ray diffraction) data were collected with a horizontal Geigerflex diffractometer on a Rigaku RU-200B rotating Cu anode at a power of 4 kW and using Ni-filtered Cu  $K\alpha$  radiation ( $\lambda = 1.542$  Å). The diffractometer is equipped with a scintillation counter. The width of the divergence, receiving, and scattering slit was 0.5°, 0.15 mm, and 0.5°, respectively. Measurements in the reflection mode covered diffraction angles ( $2\theta$ ) between 9° and 35°. The data were accumulated for 6 s at angular intervals of  $2\theta = 0.05^\circ$ .

The time-resolved WAXD measurements were performed at the DUBBLE CRG (Dutch-Belgian beamline) at the ESRF in Grenoble, France. An X-ray wavelength of 1.218 Å was used. The scattering angles at the WAXD microstrip-gas chamber detector<sup>16</sup> were calibrated with Si powder. The synthesized materials were put in small brass disks, sealed with aluminum foil, and placed in a DSC/hot stage for X-ray scattering (Linkam Scientific Ltd.). The stage was flushed with a stream of cold nitrogen gas in order to avoid sample oxidation and for thermal stability in general. Data were recorded while the sample was heated at 10 °C/min. Scattering patterns were taken every 6 s, which corresponds to one scattering pattern for each °C in the temperature ramp. The patterns were corrected for the detector response and normalized to the intensity of the primary beam measured by an ionization chamber placed upstream from the sample. The latter procedure corrects for changes in the intensity of the incoming beam and accounts for changes in sample transmission. The corrected pattern of an empty sample holder was subtracted from each pattern as a background. Finally, an additional constant background was subtracted.

Proton-decoupled solid-state  $^{13}\text{C}$  NMR spectra were recorded on a Bruker DMX500 spectrometer operating at a  $^1\text{H}$  and  $^{13}\text{C}$  NMR frequency of 500.13 and 125.13 MHz, respectively. A 4 mm magic-angle-spinning (MAS) probehead was used with sample rotation rates of 8 and 12.5 kHz. The radio-frequency power was adjusted to obtain 5  $\mu\text{s}$  90° pulses both for the  $^1\text{H}$  and  $^{13}\text{C}$  nuclei. The 38.56 ppm resonance of adamantane was used for external calibration of the  $^{13}\text{C}$  chemical shift. Proton spin–lattice relaxation in the laboratory and rotating frame,  $T_1(^1\text{H})$  and  $T_{1\rho}(^1\text{H})$ , were measured for each of the polymer components separately via cross-polarization (CP) to the  $^{13}\text{C}$  nuclei. The typical number of scans (NS) was 1024, relaxation delays in CP-derived experiments (D1) were 5 s, and the number of experiments per relaxation data set (NE) was 10.

**Table 1. Overview of Molecular Characterization of Copolyamides 12.6/12.1,4-CHDA**

entry	initial molar monomer feed ratio		molar ratio in final copolyamide		$[\eta]$ (dL g <sup>-1</sup> )
	adipic acid/ 1,4-CHDA <sup>a</sup>	cis/ trans <sup>b</sup>	adipic acid/ 1,4-CHDA <sup>b</sup>	cis/ trans <sup>b</sup>	
P.1	100/0		100/0		0.55
P.2	90/10	2/98	91/9	2/98	0.86
P.3	85/15	80/20	86/14	80/20	0.75
P.4	85/15	3/97	84/16	6/94	0.67
P.5	80/20	80/20	79/21	80/20	0.57
P.6	75/25	80/20	75/25	80/20	0.54
P.7	80/20	0/100	74/26	0/100	0.54
P.8	60/40	80/20	60/40	80/20	0.69
P.9 <sup>c</sup>	50/50	80/20	53/47	15/85	0.63

<sup>a</sup> Determined by monomer weight. <sup>b</sup> Determined by solution  $^{13}\text{C}$  NMR spectroscopy (experimental error: ca. 3%). <sup>c</sup> Synthesized with use of high-temperature/high-pressure synthetic route as described in ref 11.

For the cross-polarization-based experiments, amplitude-modulated pulses (CPramp) were utilized, being less sensitive to the experimental settings than standard CP experiments.<sup>17</sup>

### 3. Results

**Synthesis and Molecular Characterization.** Because of the possibility of isomerization of the cycloaliphatic 1,4-CHDA residues during synthesis at elevated temperature and pressure, a low-temperature solution polycondensation route with use of the more reactive acyl chloride derivatives was employed. The preservation of the initial cis/trans ratio of the 1,4-CHDA monomers was proven with solution  $^{13}\text{C}$  NMR spectroscopy. This technique was also used to determine the composition of the copolyamides 12.6/12.1,4-CHDA. The synthesis of the copolyamides and the influence of the applied synthesis conditions on the stereochemistry of the cycloaliphatic residues are discussed in more detail elsewhere.<sup>11,12</sup> The compositions and intrinsic viscosities of all samples are given in Table 1. The intrinsic viscosities of all copolyamides are comparable (0.55–0.86 dL/g). The copolymer referred to as P.9 in Table 1 was submitted to a SEC analysis to have an idea of the actual molar mass. The intrinsic viscosity of this particular sample (0.63 dL/g) is close to the average intrinsic viscosity of the samples P.1–P.8 (0.64 dL/g). For P.9 a number-average and a weight-average molecular weight of respectively 16 800 and 45 400 g/mol were obtained, which is sufficiently high to exclude a possible influence of the molecular mass on the thermal properties. This statement is supported by the data in Figure 2, as is discussed below.

**Thermal Properties.** Figure 2 shows the DSC melting points during first heating (FH) of the precipitated copolyamides 12.6/12.1,4-CHDA with 1,4-CHDA incorporated having a cis/trans ratio close to 80/20 (●) or 0/100 (○). The melting points obtained during second heating (SH), after cooling from the melt after storage for 30 min at 300 °C, are also shown for both copolyamide series (■).

Apparently, the incorporation of the more “stretched” *trans*-1,4-CHDA residues into the backbone of polyamide 12.6 results in copolyamides with a raised FH melting point, even for low degrees of incorporation of cycloaliphatic residues. In contrast, the use of 1,4-CHDA with a high cis content yields copolyamides 12.6/12.1,4-CHDA for which the FH melting points correspond remarkably well to that of polyamide 12.6.

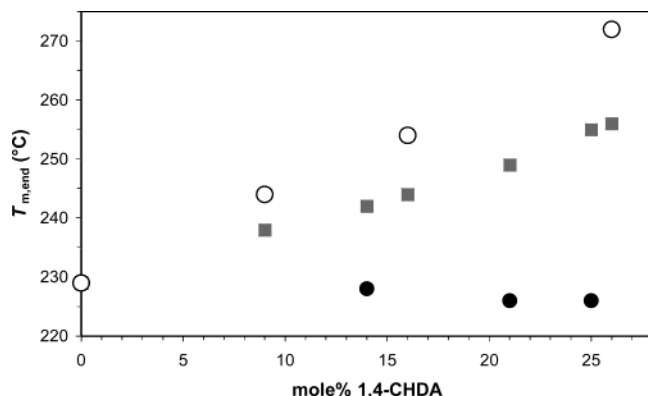


**Figure 2.** Influence of composition and stereochemistry on first and second heating melting points of copolyamides 12.6/12.1,4-CHDA. Legend: first heating melting point of initially cis-rich (●) and trans-rich (○) copolyamides. Melting point after annealing for 30 min at 300 °C (■).

The fact that the SH melting points of the copolyamides 12.6/12.1,4-CHDA are independent of the initial cis/trans ratio of the cycloaliphatic residues can be due to thermally induced isomerization. We have shown before with solution  $^{13}\text{C}$  NMR experiments that, during the thermal treatment for 30 min at 300 °C, isomerization of the 1,4-CHDA moieties, incorporated into the polyamide main chain, takes place.<sup>12,13</sup> For copolyamides based on initially *trans*-1,4-CHDA, significant amounts of the trans isomer are converted into the cis isomer, and vice versa for copolyamides based on initially high *cis*-1,4-CHDA contents. For both types of copolyamides, the cis/trans ratio is very similar after the described thermal treatment (viz.  $25 \pm 2/75 \pm 2$ ), indicating that the isomerization equilibrium has been reached. This is also illustrated in Figure 2 by the almost linear increase of the SH melting points of the copolyamides (■) with increasing contents of 1,4-CHDA residues.

If the molar masses would have been at the low side where an influence on the melting point can be expected, then a positive deviation from the straight lines could be expected for the copolyamide with 9 mol % 1,4-CHDA and an intrinsic viscosity of 0.86 dL/g, whereas a negative deviation could be expected for the sample with 26 mol % of 1,4-CHDA and an intrinsic viscosity of 0.54 dL/g. This is not observed, supporting the view that all copolyamides have a sufficiently high molar mass to have negligible effects on the melting temperatures. Perhaps superfluously it can be mentioned that Jones et al.<sup>18</sup> reported a melting point of 229 °C for a highly viscous polyamide 12.6, from which oriented fibers could be drawn, which requires high molecular weight material. This melting point is very close to the value for our polyamide 12.6 with an intrinsic viscosity of 0.55 dL/g, being one of the lowest viscosities in the series of copolyamides.

**Room Temperature WAXD Analysis.** The WAXD pattern of semicrystalline polymers generally consists of distinctive, more-or-less sharp diffraction signals from the crystalline phase, superimposed on a broad halo originating from the noncrystalline phase. For most polyamides, two characteristic diffraction signals, at spacings around 0.44 and 0.37 nm, can be distinguished. The former diffraction signal (indexed 100) yields information about the interchain distance within a hydrogen-bonded sheet, whereas the latter (a superposition of 010 and 110 reflections) can provide insight into

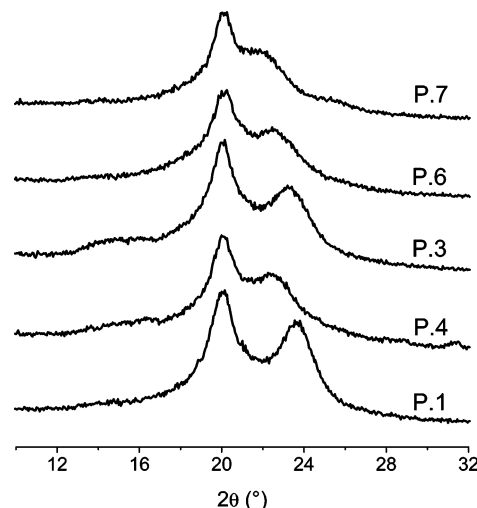


**Figure 3.** Room temperature WAXD analysis of "as-synthesized" copolyamides 12.6/12.1,4-CHDA as a function of composition ( $\lambda = 1.542$  Å). Legend: (P.1) polyamide 12.6; (P.4) 16 mol % 1,4-CHDA (cis/trans: 6/94); (P.3) 14 mol % 1,4-CHDA (cis/trans: 80/20); (P.6) 25 mol % 1,4-CHDA (cis/trans: 80/20), and (P.7) 26 mol % 1,4-CHDA (cis/trans: 0/100). (The curves were shifted along the y-axis for clarity.)

the distance between the separate sheets.<sup>18</sup> As a result and given Bragg's law, it is possible to interpret the WAXD data obtained for the copolyamides 12.6/12.1,4-CHDA in terms of interchain and intersheet distances.

The diffraction pattern obtained for polyamide 12.6 (see Figure 3, curve P.1) clearly displays the two typical reflections at a diffraction angle of 20.14° and 23.60° (corresponding to spacings of 0.441 and 0.377 nm, respectively). The interchain distances are controlled by hydrogen bonding and are larger than the van der Waals determined intersheet distances.

As can be deduced from Figure 3, the 100 reflections (around  $2\theta = 20^\circ$ ) and hence the interchain distances are almost invariant upon the partial substitution of the adipic acid with 1,4-CHDA residues. In contrast, the combined 010 and 110 reflection (around  $2\theta = 22\text{--}24^\circ$ ) shifts to lower diffraction angles upon substitution of adipic acid with *trans*-1,4-CHDA residues. For the *trans*-rich 1,4-CHDA-containing polyamides (curves P.4 and P.7), the intersheet distance ( $d$ ) increases with an increasing content in cycloaliphatic residues [polyamide 12.6 (P.1),  $d = 0.377$  nm; copolyamide 12.6/12.1,4-CHDA (84/16; cis/trans: 6/94; P.4),  $d = 0.399$  nm; copolyamide 12.6/12.1,4-CHDA (74/26; cis/trans: 0/100; P.7),  $d = 0.407$  nm]. Use of 1,4-CHDA with a high cis isomer content yields copolyamides for which the diffraction patterns are comparable to that of polyamide 12.6 (curves P.3 and P.6). This difference between cis and trans comonomers is most clear when comparing the intersheet distances of a copolyamide 12.6/12.1,4-CHDA with 16 mol % 1,4-CHDA and a cis/trans ratio of 6/94 (curve P.4;  $d$ : 0.399 nm), with the copolyamide that contains 14 mol % 1,4-CHDA but with a cis/trans ratio of 80/20 (curve P.3;  $d$ : 0.383 nm).

**Temperature-Dependent WAXD Analysis.** It is known that when polyamide crystals are heated, the spacings of the two characteristic diffraction signals shift toward one another and merge at the Brill temperature ( $T_B$ ) to a Brill spacing of ca. 0.42 nm.<sup>19</sup> Occasionally, this single diffraction signal remains until melting ( $T_m$ ) and the corresponding spacing only increases slightly as a consequence of thermal expansion.



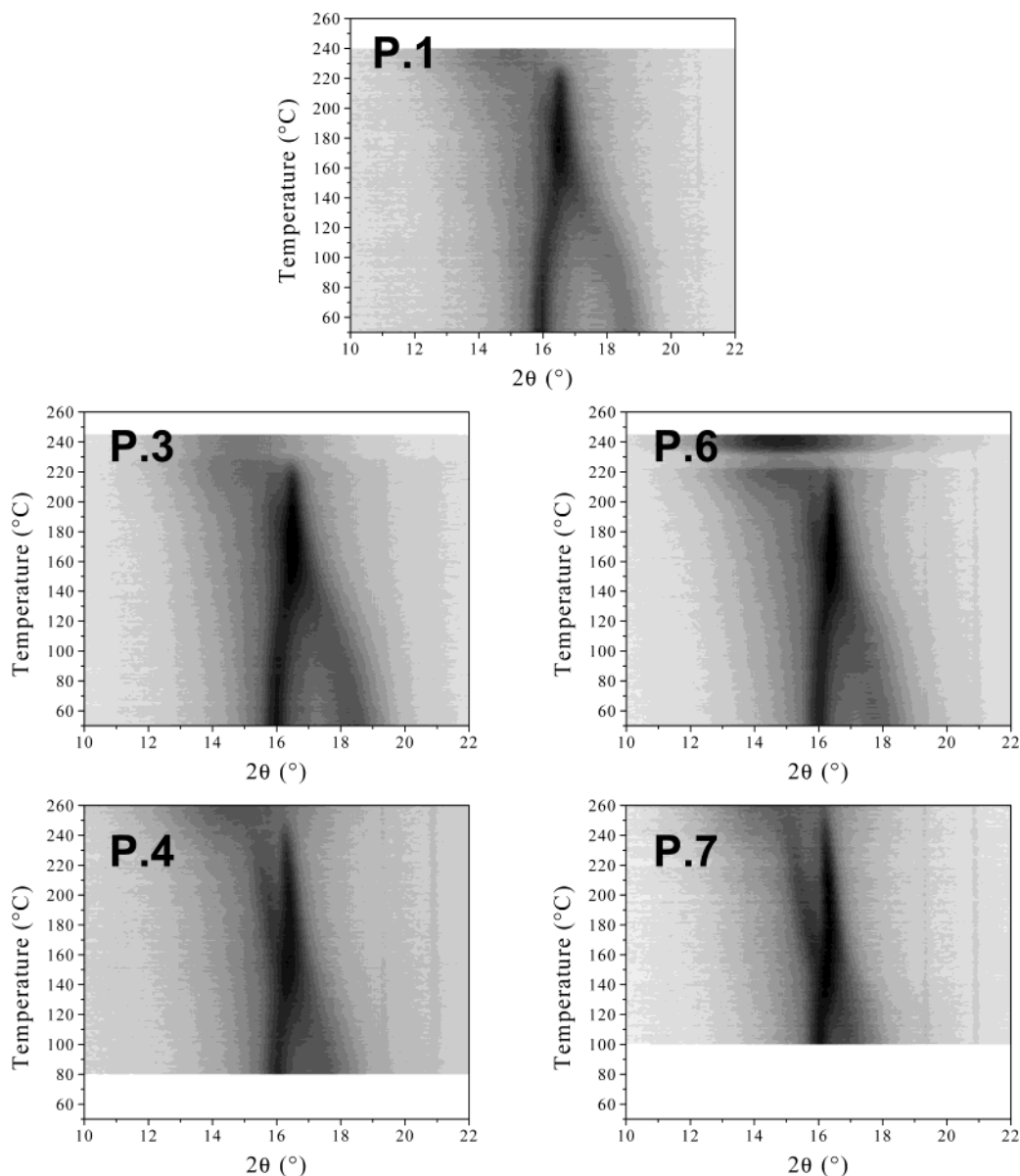


**Figure 4.** Temperature-dependent WAXD data during the first heating of copolyamides 12.6/12.1,4-CHDA ( $\lambda = 1.218 \text{ \AA}$ ). Legend: (P.1) polyamide 12.6; (P.3) 14 mol % 1,4-CHDA (cis/trans: 80/20); (P.6) 25 mol % 1,4-CHDA (cis/trans: 80/20); (P.4) 16 mol % 1,4-CHDA (cis/trans: 6/94), and (P.7) 26 mol % 1,4-CHDA (cis/trans: 0/100). (The starting temperature of all samples was adjusted to give all samples the same exposure time. The actual temperature window of a given sample depends on the expected final melting of the copolyamide.)

The high-temperature crystalline phase between  $T_B$  and  $T_m$ , for which the interchain and the intersheet distances have become equal, is often referred to as pseudo-hexagonal.<sup>18–27</sup>

WAXD patterns of the copolyamides discussed in this paper were collected during heating by using synchrotron radiation. Only first heating runs are reported since the thermally induced isomerization changes the cis/trans ratio. Figure 4 shows the scattering patterns as a function of temperature (with the scattered intensity represented with a gray scaling) for the different (co)-polyamides.

The crystalline reflections of polyamide 12.6 (Figure 4, P.1) behave as expected. The diffraction signals at 0.438 and 0.377 nm merge upon heating to a common reflection corresponding to a distance of 0.424 nm at 160 °C ( $= T_B$ ). At higher temperatures, the pseudo-hexagonal crystals melt, and concomitantly the liquidlike scattering of the amorphous phase (the amorphous halo)

grows to its maximum size. Occasionally the samples leaked out of the holders upon melting, resulting in an apparent extinction of the sample's scattering at these temperatures. The shift of the intersheet distance as a function of the temperature is much more pronounced compared to that of the interchain distance.

Clearly, the scattering patterns of the copolyamides 12.6/12.1,4-CHDA that were synthesized using 1,4-CHDA with a high cis isomer content (Figure 4, P.3 and P.6) show a temperature dependence similar to that of the polyamide 12.6 (Figure 4, P.1). In contrast, incorporation of 1,4-CHDA with a high trans isomer content yields a quite different evolution of the scattering patterns upon heating (Figure 4, P.4 and P.7), showing crossing diffraction signals upon heating, rather than merging ones. To the best of our knowledge, such a crossing of diffraction signals has not been reported before for polyamides. It points at the inability of

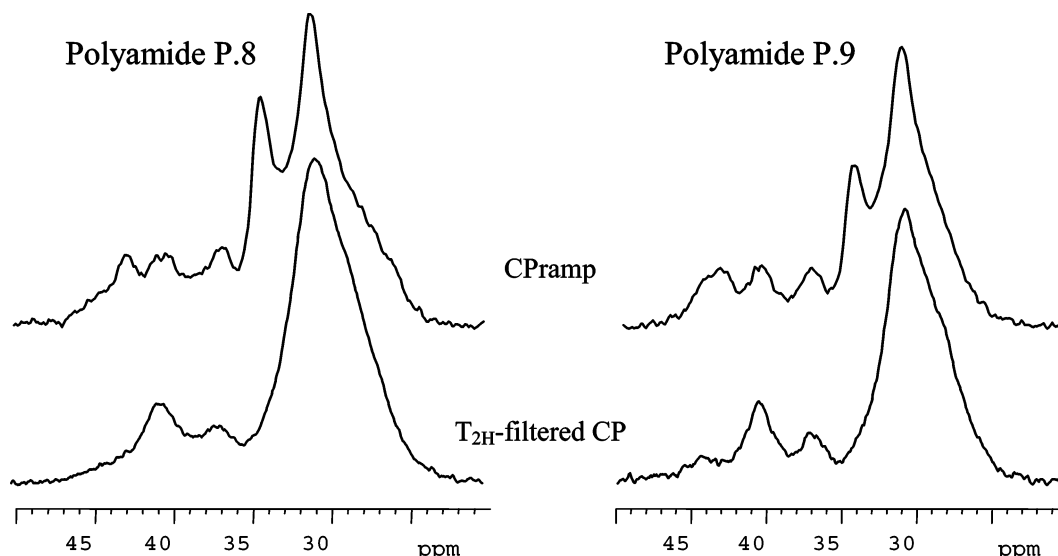


**Figure 5.** Comparison of regular CPramp and  $T_{2H}$ -filtered CP experiments for a cis-rich (polyamide P.8) and a trans-rich copolyamide 12.6/12.1,4-CHDA (polyamide P.9).

forming a pseudohexagonal phase in this particular case.

**Solid-State NMR Analysis.** Solid-state  $^1\text{H}$  and  $^{13}\text{C}$  NMR spectroscopy is a powerful technique to study the nanostructure and chain dynamics of polymers.<sup>28</sup>  $^1\text{H}$  NMR line shapes and relaxation are particularly informative about chain mobility and phase separation in the solid polymers. High-power proton-decoupled magic-angle spinning (MAS)  $^{13}\text{C}$  NMR spectroscopy offers sufficient resolution to distinguish between resonances of chemical distinct carbon atoms in the primary polymer structure or even between chemically identical carbons in different polymer phases. By use of cross-polarization (CP) the two can be joined together into a so-called wide-line-separation (WISE) experiment,<sup>29</sup> a two-dimensional  $^1\text{H}$ - $^{13}\text{C}$  NMR technique which combines the resolution along the  $^{13}\text{C}$  axis and the mobility information along the  $^1\text{H}$  axis. In the present solid-state NMR investigation, we have studied  $^1\text{H}$  NMR spin-lattice relaxation in the laboratory and rotating frame ( $T_1$  and  $T_{1\rho}$ ) through the well-resolved signals in the  $^{13}\text{C}$  NMR spectrum (e.g., signals of either crystalline or amorphous domains) to determine the relationship between the configuration of the cycloaliphatic residues in copolyamides 12.6/12.1,4-CHDA and their location in either the crystalline or the amorphous phase.

For these solid-state NMR experiments we chose two copolyamides 12.6/12.1,4-CHDA with quite comparable contents in 1,4-CHDA residues (40 and 47 mol %, respectively), but different cis/trans ratios (80/20 and 15/85, respectively) (see Table 1, entries P.8 and P.9).

Despite the use of high-power proton decoupling and magic-angle-spinning, the signals in the MAS  $^{13}\text{C}$  NMR spectra of the two copolyamides 12.6/12.1,4-CHDA are (Figures 5 and 6) still much broader than in the solution spectra (not shown). This is a result of heterogeneity, local susceptibility variation, and conformational distributions that may exist within the solid, but in solution would be averaged out by motions. The solid-state NMR spectra are more than a broadened version of the solution NMR spectra. Additional signal intensity at 34 and 44 ppm is observed in  $^1\text{H}$ - $^{13}\text{C}$  cross-polarization spectra and, to a less extent, direct-excitation  $^{13}\text{C}$  NMR spectra. By analogy with the MAS  $^{13}\text{C}$  NMR spectrum of polyethylene,<sup>29</sup> we assign these additional

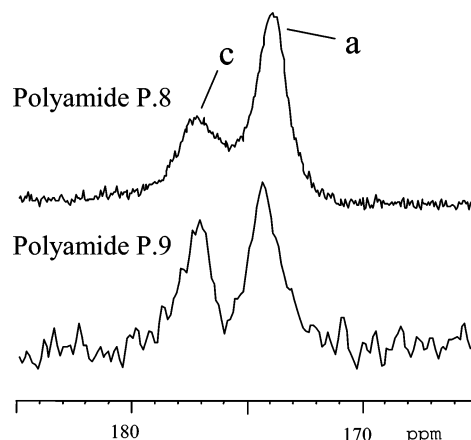


**Figure 6.** Carbonyl region in the CPMAS  $^{13}\text{C}$  NMR spectra of the cis-rich copolyamide P.8 and the trans-rich copolyamide P.9 (c: 1,4-CHDA; a: adipic acid).

signals to the crystalline phase. Indeed,  $T_{2H}$ -filtered CP spectra (Figure 5) show that the signals at 34 and 44 ppm belong to a rigid fraction of the polyamide.

Proton spin-lattice relaxations in rotating and laboratory frame measurements ( $^1\text{H}$   $T_{1\rho}$  and  $T_1$ ) yield mobility information in the kilohertz and gigahertz regime, respectively. In addition, and importantly for polymer NMR spectroscopy, they provide information about the miscibility and domain sizes of various phases inside the polymer. If the average domain size in a polymer blend is smaller than ca. 1 nm, proton-proton spin diffusion averages out any  $T_{1\rho}$  or  $T_1$  relaxation difference. All protons decay with the same effective  $T_{1\rho}$  and  $T_1$ . In contrast, if the domain size is larger than ca. 50 nm, spin diffusion is too slow to average out such differences, and the phases will decay each with their intrinsic, probably different  $T_{1\rho}$  and  $T_1$  values. In the intermediate range, 1 nm < domain size < 50 nm, we expect to find different effective  $T_{1\rho}$  values and a single effective  $T_1$ . The reason is that  $T_1$  tends to be 10–100 times longer than  $T_{1\rho}$ , so that spin diffusion, though unable to homogenize  $T_{1\rho}$ , is still able to average out  $T_1$  differences.

The  $T_{1\rho}$  and  $T_1$  data for the cis- and trans-rich copolyamide show exactly such intermediate behavior.

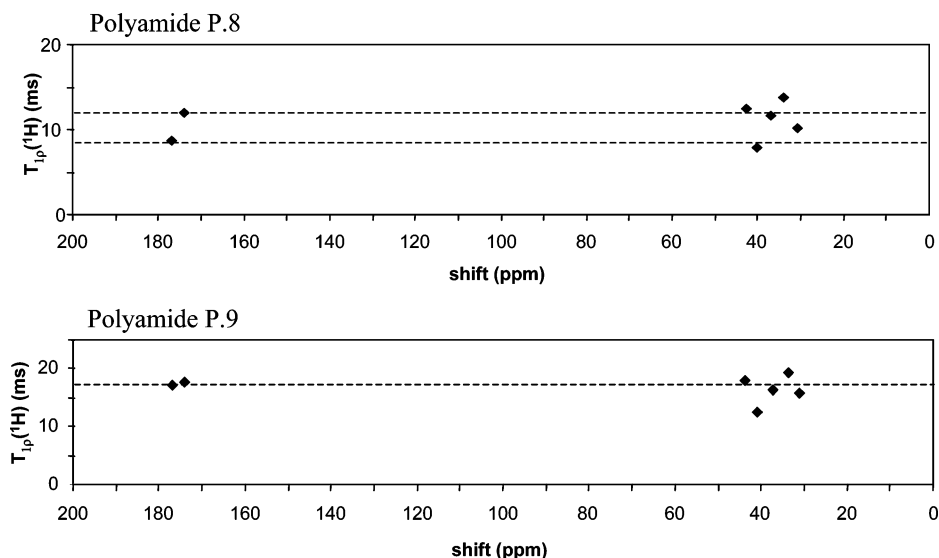


**Figure 7.** Proton  $T_{1\rho}$  measurements performed on a cis-rich (polyamide P.8) and trans-rich copolyamide 12.6/12.1,4-CHDA (polyamide P.9).

The signals at 34 and 44 ppm have a significantly longer  $T_{1\rho}$  than the others (Figure 7), whereas all resonances show similar  $T_1$  values in the range 1.2–1.3 s. In combination with our peak assignment, this indicates that the crystalline domains are between 1 and 50 nm in size. For a common proton spin-diffusion coefficient of ca. 1 nm<sup>2</sup>/s, this would agree with the typical lamellar thickness of polyamides of about 5 nm.<sup>18</sup>

Interestingly,  $T_{1\rho}$  values obtained for the cis-rich copolyamide (polyamide P.8) are significantly lower than for the trans-rich copolyamide (polyamide P.9), indicating more rotational mobility in the low-frequency regime for the cis-rich than for the trans-rich copolyamide (Figure 7). Since the two polyamides show the same  $T_1$  behavior, there appears to be no significant mobility difference in the gigahertz regime probably associated with local chain motions.

With regard to the question of whether 1,4-CHDA is located in the crystalline or amorphous domains, the peak at 177 ppm (Figure 6) is of special interest because it is assigned to this moiety. For the trans-rich copolyamide (Figure 7, polyamide P.9), the  $T_{1\rho}$  values found for both the 1,4-CHDA (177 ppm) and adipic acid residues (174 ppm) are similar and in between the values found for signals corresponding to the amorphous (e.g., 31 ppm) or crystalline phases (e.g., 34 ppm). In contrast, for a cis-rich copolyamide (Figure 7, polyamide P.8) the  $T_{1\rho}$  value of the 1,4-CHDA residues (177 ppm) is significantly lower than the value found for the adipic acid residues (174 ppm). Moreover, the value found for the (mainly cis) cycloaliphatic residues is in good agreement with the  $T_{1\rho}$  value of signals assigned to the amorphous phase. In this way, we have shown that the location of the 1,4-CHDA residues (amorphous/crystalline) is dependent on the configuration of the cycloaliphatic moieties. As expected, repeating units containing the “kinky” *cis*-1,4-CHDA residues are not incorporated into the crystalline phase and are located in the amorphous regions only. *trans*-1,4-CHDA, as well as adipic acid residues, shows a  $T_{1\rho}$  behavior in between that of the amorphous and crystalline moieties and consequently are present in both the crystalline and amorphous domains.

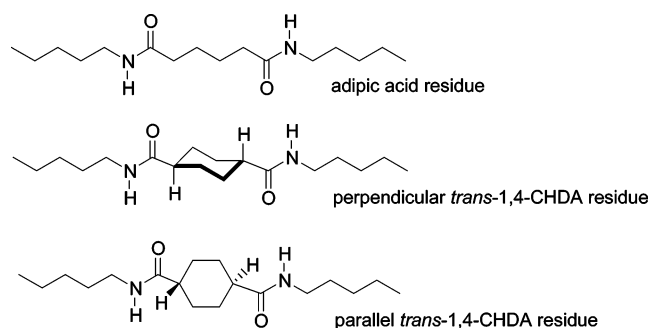


**Figure 8.** Comparison of the perpendicular or parallel incorporation of *trans*-1,4-CHDA residues, with respect to the plane of the polyamide chain.

#### 4. Discussion

Given the strong solid-state NMR evidence for the incorporation of the *trans* cycloaliphatic residues and the absence of *cis* residues inside the crystals, it is possible to rationalize the WAXD and DSC data.

Clearly the incorporation of the *trans*-1,4-CHDA residues gives rise to a unit cell expansion predominantly by enlarging the intersheet distance without affecting the interchain distance. Consequently, the incorporated cyclohexane ring is most likely oriented perpendicular to the plane of the hydrogen-bonded polymer chains as represented in Figure 8.

The small but observable shift in the intersheet distance for a copolyamide containing 25 mol % 1,4-CHDA residues with a high *cis* isomer content (*cis*/*trans*: 80/20; curve P.6 in Figure 3) can be attributed to the presence of a small, but not negligible, amount of *trans*-1,4-CHDA residues; that is able to be incorporated into the crystalline regions. In the case of 25 mol % 80/20 *cis*/*trans* 1,4-CHDA residues (curve P.6), the total amount of *trans* isomer, available for incorporation, is obviously much higher than in the case of 14 mol % 80/20 *cis*/*trans* 1,4-CHDA residues (curve P.3).

The *trans*-1,4-CHDA-containing copolyamide crystals do not melt from the pseudohexagonal phase, as usually reported for even–even polyamides.<sup>18,20</sup> Some polyamides have Brill temperatures lower than their  $T_m$  (e.g., polyamides 6.6,<sup>18,21</sup> 4.6,<sup>24</sup> 6.8,<sup>24</sup> 4.4, 6.4, 8.4, 10.4, and 12.4<sup>25</sup>), whereas for others the  $T_B$  and  $T_m$  are



coincident (e.g., 4.8, 4.10, 4.12, 6.10, 6.12, 6.18, and 8.12<sup>20</sup>). Jones et al.<sup>20</sup> suggested that the increased torsional flexibility of the alkane segments above  $T_B$  exerts a torsional force on the more rigid amide groups and that some of them break, flip out by ca. 60° or even ca. 120°, and reassociate to form a three-dimensional network of intra- and intersheet hydrogen bonds. These intersheet hydrogen bonds pin the nylon chains onto the pseudohexagonal lattice sites and prevent the chains from moving further apart. In this way, the intersheet and interchain distances become equal and more or less fixed for further expansion, resulting in the pseudohexagonal phase. According to this view, a reduction of the rotational mobility of the amide bonds attached to cycloaliphatic residues may well hamper the flipping of the amide bonds out of the hydrogen-bonded sheets and hence prevent the formation of intersheet hydrogen bonds. In this way, transformation into the pseudohexagonal phase would be prevented, and the intersheet distance (controlled by van der Waals interactions) would further increase with temperature, whereas the interchain distance would remain more or less constant (controlled by hydrogen bonding). However, this scenario conflicts with NMR<sup>30–32</sup> data in the case of polyamide 6.6 and infrared (IR) measurements<sup>33</sup> in the case of nylon 6.10, 6.12, and 10.10, demonstrating that the hydrogen bonds are maintained until the onset of melting. In fact, the IR data do not exclude the hydrogen bond flipping option as melt-crystallized polyamide 6.10, 6.12, and 10.10 do not display a pseudohexagonal phase prior to melting. In contrast, the mentioned polyamide 6.6 NMR report includes data up to 228 °C, which is above the  $T_B$  of 190 °C, and rules out the possibility of continuous hydrogen bond flipping in the pseudohexagonal phase. If the behavior of polyamide 6.6 is representative for all aliphatic polyamides, it cannot be taken for granted that—thinking in terms of Jones et al.—the pseudohexagonal phase involves the breaking of some of the interchain hydrogen-bonding concomitant to the formation of intersheet hydrogen bonds<sup>20</sup> and that a reduction of the rotational mobility of the amide bonds attached to cycloaliphatic residues is an explanation for the absence of such a phase in the case of copolyamides with cyclic residues in their crystalline domains. Alternatively, it could be that the presence of rigid cyclic residues lowers the symmetry needed for a pseudohexagonal phase, which in the case of linear aliphatic residues is accomplished by the temperature-induced conformational disordering of the methylene sequences.<sup>34</sup>

The raise in  $T_m$  of the copolyamides with predominantly *trans*-1,4-CHDA residues supports their incorporation into the crystalline phase as a *solid solution* rather than as defects, as the latter would lower the melting temperature. In the case of a solid solution the melting point (solid–liquid line) varies gradually with the crystal composition from that of one pure component to that of the other. A rough estimate of the melting point of polyamide 12.*trans*-1,4-CHDA can be made by linear extrapolation of the open circles to a sample with 100% 1,4-CHDA in Figure 2 and amounts to 395 °C. This value, however, is merely indicative. In addition, the DSC results are compatible with the total exclusion of the *cis* moieties since the FH melting points of *cis*-rich copolyamides are a little lower than that of polyamide 12.6 and lower with increasing comonomer content. The melting point depression due to the pres-

ence of dilutents (or comonomer) in the case of polymers is not expected to be very large. Solid solution and melting point depression effects both determine the actual melting temperature of copolymers with mixed *cis* and *trans* moieties.

It should be remarked that the conclusions presented above are derived from experimental rather than equilibrium melting points, thus neglecting effects that are related to crystal size, surface structure, or enthalpic differences between the crystals. Most of these parameters can be tuned by changing the thermal history of a given sample. In the case of polyamide 12.6 such changes are mostly visible in the shape and peak of the melting traces whereas the endset is hardly affected. Expecting a similar behavior for the copolymers, the endset temperatures were used in the present work. Tuning the thermal history of the copolymers was not an option in the present case, since any residence time at high temperatures alters the *cis*/*trans* ratio of the comonomers. For sure the melting point increase due to the incorporation of *trans* moieties cannot be reached by changing the crystallization conditions of nylon 12.6. Finally, the SH DSC data in Figure 2 demonstrate that the fast cooling procedure applied before running a FH experiment is not imperative for the formation of the solid solution. A melting point increase is also observed after cooling rather slowly at 10 °C/min, although less pronounced due to isomerization.

## 5. Conclusions

The configuration of the cycloaliphatic residues in the copolyamides 12.6/12.1,4-CHDA is the determining factor in the cocrystallization of linear and cyclic aliphatic residues. The “stretched” *trans* isomers readily cocrystallize with the adipic acid residues as a solid solution rather than as defects, thereby increasing the melting point and expanding the room temperature crystalline structure. In contrast, introduction of *cis* isomers into the polymer main chain leads to a moderate melting point depression without affecting the crystalline structure of the copolyamides, indicating the repulsion of these moieties from the crystalline phase as could independently be deduced from solid-state NMR data. Finally, the presence of *trans* cycloaliphatic residues in the crystalline phase prevents the formation of a pseudohexagonal phase during heating prior to melting. In other words, for these samples a classical Brill transition does not exist, and a crossing rather than a merging of the WAXD crystalline reflections is observed.

**Acknowledgment.** The authors acknowledge Prof. Dr. Ir. B. Van Mele and Ir. S. Swier (both FYSC, Free University of Brussels; VUB) for their help in the thermal characterization. B. Vanhaecht is very grateful to the Fund for Scientific Research–Flanders (Belgium) (F.W.O.) for financing his Ph.D. study. B. Goderis is a postdoctoral fellow of the Fund for Scientific Research–Flanders and acknowledges support by FWO–Flanders in the framework of the DUBBLE project (G.0177.03). M. Biesemans and R. Willem acknowledge support from the Fund for Scientific Research–Flanders (Belgium, Grants G.0192.98 and G.0016.02).

## References and Notes

- (1) Kricheldorf, H. R.; Schwarz, G. *Makromol. Chem.* **1987**, *188*, 1281.

- (2) Tenkovtsev, A. V.; Rutman, A. B.; Bilibin, Yu, A. *Makromol. Chem.* **1992**, *193*, 687.
- (3) Osman, M. A. *Macromolecules* **1986**, *19*, 1824.
- (4) Kwolek, S. L.; Luise, R. R. *Macromolecules* **1986**, *19*, 1789.
- (5) Reck, B.; Ringsdorf, H.; Gardner, K.; Starkweather, H., Jr. *Makromol. Chem.* **1989**, *190*, 2511.
- (6) Srinivasan, R.; Prasad, A.; Marand, H.; McGrath, J. E. *Polym. Prepr. (Am. Chem. Soc., Div. Polym. Chem.)* **1991**, *32*, 174.
- (7) Srinivasan, R.; McGrath, J. E. *Polym. Prepr. (Am. Chem. Soc., Div. Polym. Chem.)* **1992**, *33*, 503.
- (8) Srinivasan, R.; Moy, T.; Saikumar, J.; McGrath, J. E. *Polym. Prepr. (Am. Chem. Soc., Div. Polym. Chem.)* **1992**, *33*, 225.
- (9) Ridgway, J. S. *J. Polym. Sci., Part A-1* **1970**, *8*, 3089.
- (10) Kalmykova, V. D.; Bogdanov, M. N.; Okromchedlidze, N. P.; Zhmayeva, I. V.; Yefremov, Ya, V. *Polym. Sci. USSR* **1967**, *9*, 2539.
- (11) Vanhaecht, B.; Teerenstra, M. N.; Suwier, D. R.; Willem, R.; Biesemans, M.; Koning, C. E. *J. Polym. Sci., Polym. Chem.* **2001**, *39*, 833.
- (12) Vanhaecht, B.; Rimez, B.; Willem, R.; Biesemans, M.; Koning, C. E. *J. Polym. Sci., Polym. Chem.* **2002**, *40*, 1962.
- (13) Koning, C.; Vanhaecht, B.; Willem, R.; Biesemans, M.; Goderis, B.; Rimez, B. *Macromol. Symp.* **2003**, *199*, 431.
- (14) Koning, C.; Vanhaecht, B.; Willem, R.; Biesemans, M.; Goderis, B.; Rimez, B. *Polym. Prepr. (Am. Chem. Soc., Div. Polym. Chem.)* **2003**, *44*, 1063.
- (15) Laatikainen, R.; Niemitz, M.; Malaisse, W. J.; Biesemans, M.; Willem, R. *Magn. Res. Med.* **1996**, *36*, 359.
- (16) Zhukov, V.; Udo, F.; Marchena, O.; Hartjes, F. G.; van den Berg, F. D.; Bras, W.; Vlieg, E. *Nucl. Instrum. Methods A* **1997**, *392*, 83.
- (17) Verel, R.; Baldus, M.; Nijman, M.; Van Os, J. W. M.; Meier, B. H. *Chem. Phys. Lett.* **1997**, *280*, 31.
- (18) Jones, N. A.; Cooper, S. J.; Atkins, E. D. T.; Hill, M. J.; Franco, L. *J. Polym. Sci., Polym. Phys. Ed.* **1997**, *35*, 675.
- (19) Brill, R. *Z. Phys. Chem. (Munich)* **1943**, *61*, 1353.
- (20) Jones, N. A.; Atkins, E. D. T.; Hill, M. J.; Cooper, S. J.; Franco, L. *Polymer* **1997**, *38*, 2689.
- (21) Starkweather, H. W.; Whitney, J. F.; Johnson, D. R. *J. Polym. Sci., Polym. Phys. Ed.* **1963**, *1*, 715.
- (22) Sandeman, I.; Keller, A. *J. Polym. Sci.* **1956**, *19*, 401.
- (23) Ramesh, C.; Keller, A.; Eltink, S. J. E. A. *Polymer* **1994**, *35*, 2483.
- (24) Hill, M. J.; Atkins, E. D. T. *Macromolecules* **1995**, *28*, 604.
- (25) Jones, N. A.; Atkins, E. D. T.; Hill, M. J.; Cooper, S. J.; Franco, L. *Macromolecules* **1996**, *29*, 6011.
- (26) Jones, N. A.; Atkins, E. D. T.; Hill, M. J.; Cooper, S. J.; Franco, L. *Macromolecules* **1997**, *30*, 3569.
- (27) Atkins, E. D. T.; Hill, M. J.; Jones, N. A.; Cooper, S. J. *J. Polym. Sci., Polym. Phys. Ed.* **1998**, *36*, 2401.
- (28) Kohan, M. I. *Nylon Plastics Handbook*; Hanser Publishers: Munich, 1995; Chapter 4, p 94.
- (29) Schmidt-Rohr, K.; Spiess, H. W. *Multidimensional Solid-State NMR and Polymers*; Academic Press: London, 1994; Chapter 7.
- (30) Flory, P. J.; Williams, A. D. *J. Polym. Sci., Part A2* **1967**, *5*, 399.
- (31) Hirschinger, J.; Miura, H.; Gardner, K. H.; English, A. D. *Macromolecules* **1990**, *23*, 2153.
- (32) Wendoloski, J. M.; Gardner, K. H.; Hirschinger, J.; Miura, H.; English, A. D. *Science* **1990**, *247*, 431.
- (33) Yoshioka, Y.; Tashiro, K.; Ramesh, C. *Polymer* **2003**, *44*, 6407.
- (34) Yoshioka, Y.; Tashiro, K. *Polymer* **2003**, *44*, 7007.

MA035103R